Chinese Chemical Letters 33 (2022) 4846–4849

Contents lists available at ScienceDirect

Chinese Chemical Letters

journal homepage: www.elsevier.com/locate/cclet

Polymerization of pyrrole induced by pillar[5]arene functionalized graphene for supercapacitor electrode

Fang Guo[a], Junqiang Guo[a], Zhiqiang Zheng[a], Tao Xia[a], Aadil Nabi Chishti[a], Liwei Lin[a], Wang Zhang[a,b,*], Guowang Diao[a]

[a] School of Chemistry and Chemical Engineering, Yangzhou University, Yangzhou 225002, China
[b] Department of Applied Bioengineering, Graduate School of Convergence Science and Technology, Seoul National University, Suwon 443-270, South Korea

ARTICLE INFO

Article history:
Received 21 October 2021
Revised 25 January 2022
Accepted 27 January 2022
Available online 14 February 2022

Keywords:
Nanocomposite
Pillar[5]arene
Graphene
Polypyrrole
Supercapacitor

ABSTRACT

Conducting polymer is an important electrode material for supercapacitors because of its high initial specific capacitance. Herein, a novel nanocomposite composed of polypyrrole (PPy) film homogeneously immobilized on the pillar[5]arene functionalized reduced graphene oxide nanosheets (RGO-HP5A-PPy) was successfully prepared. RGO-HP5A induced pyrrole to polymerize on the graphene surface and the specific capacitance loss caused by PPy agglomeration was avoided. Noticeably, the specific capacitance of RGO-HP5A-PPy was up to 495 F/g at 1 A/g. Compared with pure PPy (319 F/g), the specific capacitance was increased by 55%. The specific capacitance retention of the assembled symmetric supercapacitor reached 76% after 10,000 cycles at 5 A/g. This study gave full play to the advantages of pillar[5]arene, graphene and PPy, and was expected to promote the development of supramolecular functionalized composites in energy storage.

Supercapacitors have the advantages of high power density, almost no maintenance, no memory effect and good safety [1–4]. The relevant studies have attracted much attention in the field of electrochemistry. Electrode materials play a decisive role in the performance of supercapacitors, so it is very important to improve the electrochemical performance of electrode materials. Conducting polymer is a promising pseudocapacitive material with high initial specific capacitance, good conductivity and low cost [5–8]. However, pure conducting polymers tend to aggregate when used as electrode materials, reducing the effective transport path of ions [9,10]. Therefore, researchers often combine polymers with other materials to alleviate agglomeration and improve their electrochemical properties [11,12]. As an important member of the conducting polymer family, polypyrrole (PPy) has relatively good chemical and thermal stability [13,14]. However, like other conducting polymers, PPy has poor cyclic stability and its specific capacitance will be greatly attenuated due to polymer chain fracture during continuous charge and discharge [15,16]. It is necessary to find materials with good conductivity and stability to compound with PPy for better electrochemical performance.

Graphene has been widely reported as an electrode material, described as far superior to existing carbon- and polymer-based materials for supercapacitors [17–19]. However, the specific capacitance of graphene is not as high as expected due to the restacking of graphene nanosheets caused by van der Waals interactions [19,20]. Surface modification and the introduction of intercalated materials are commonly used to inhibit stacking [21,22]. For example, using pillar[5]arenes (supramolecular macrocyclic compounds with pillar shape [23–26]) to modify graphene could effectively inhibit the aggregation of graphene nanosheets. Our group used to modify amphiphilic pillar[5]arenes onto the surface of reduced graphene oxide (RGO) to prepare a water-dispersible nanocomposite, which had selective supramolecular recognition and enrichment for guest molecules [27]. After that, a hydrazide-pillar[5]arene functionalized reduced graphene oxide (RGO-HP5A) for supercapacitor electrode with high specific capacitance, good rate capability and long cycle life was prepared *via* the reduction of graphene oxide (GO) by hydrazide-pillar[5]arene (HP5A) [28]. In addition, loading conducting polymers on the surface of graphene could also inhibit the re-stacking of graphene nanosheets and easily form disordered nanosheets with porous structure, which increased the surface area of composite materials and provided channels for ion diffusion [29,30]. With graphene as a support, conducting polymers improved both their conductivity and cycling stability. The researchers synthesized conducting polymers/graphene hybrid structures through various approaches, such as initiating polymerization on the surface of GO [31] and RGO

* Corresponding author.
E-mail address: zhangwang@yzu.edu.cn (W. Zhang).

https://doi.org/10.1016/j.cclet.2022.01.088
1001-8417/

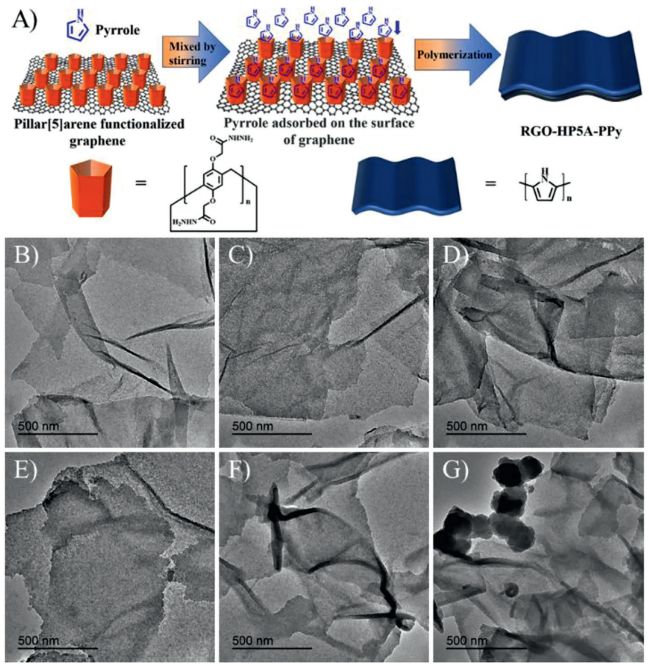

Fig. 1. (A) Schematic of the synthesis process of RGO-HP5A-PPy composites. TEM images of (B) RGO-HP5A-PPy 1–1, (C) RGO-HP5A-PPy 1–2, (D) RGO-HP5A-PPy 1–3, (E) RGO-HP5A-PPy 1–4, (F) RGO-HP5A-PPy 1–5 and (G) RGO-HP5A-PPy 1–6.

[32], preparing by electrochemical deposition [33] and chemical vapor deposition (CVD) polymerization [34]. Although these studies have indeed improved a certain property of the material (one of capacitance or cycle life), it often results in a decrease in other aspects of the material's performance. One of the important reasons is that the components are not tightly combined. Therefore, it is still an important topic to find a more simple and effective method to synthesize conducting polymer/graphene hybrid materials with stable structures.

Herein, we utilized pillar[5]arene functionalized graphene as the substrate to induce pyrrole to polymerize on the surface of graphene (mainly due to the enrichment ability of pillar[5]arenes on RGO-HP5A for guest molecules) to prepare graphene-pillar[5]arene-polypyrrole ternary composites (RGO-HP5A-PPy) as supercapacitor electrode materials. The PPy in the composite was uniformly covered on the graphene surface in the form of a film, compared with the pure PPy prepared by a similar method in the form of particles. Our synthesis strategy simplified the conventional preparation process of PPy-based film composites, because it did not require multi-step reactions or additional dispersant agents. The obtained RGO-HP5A-PPy composites with good hydrophilicity had a maximum specific capacitance of 495 F/g (RGO-HP5A-PPy 1–5) at the current density of 1 A/g, which was 55% higher than that of pure PPy (319 F/g). Meanwhile, the rate capability of RGO-HP5A-PPy 1–5 in the range of 1∼20 A/g was improved obviously, which was increased by 150% compared with that of PPy.

The novel RGO-HP5A-PPy composites were prepared by free-radical polymerization of pyrrole (see Experimental section in Supporting information for details). The main process of preparation was shown in Fig. 1, where pyrrole was added in an aqueous dispersion of RGO-HP5A and adsorbed on the surface of RGO-HP5A through supramolecular complexation of pillar[5]arene with pyrrole [35,36]. Then, ammonium persulfate (APS) acted as a radical initiator and was dropped into the aqueous dispersion. Both the pyrrole in the cavity of pillar[5]arenes and free pyrrole in the solution could polymerize. Due to the relatively higher concentration of pyrrole on the graphene surface, the pyrrole adsorbed on the graphene surface polymerized [36]. The formed PPy covered the graphene and caused a decrease in the concentration of pyrrole here. The concentration gradient induced the free pyrrole in the reaction mixture diffusing to the surface of the graphene, so that the PPy layer continued to grow.

The morphology and microstructure of the composites were investigated by transmission electron microscopy (TEM) and scanning electron microscopy (SEM). Figs. 1B-G showed the TEM images of RGO-HP5A-PPy composites, where graphene maintained a thin sheet shape during the polymerization of pyrrole. Figs. 1B-F exhibited that PPy was uniformly loaded on the surface of graphene in a thin film form, and the thickness of the lamella increased gradually with the increase of the amount of pyrrole added, indicating that RGO-HP5A could induce the polymerization of pyrrole on the graphene. However, pyrrole would polymerize outside the graphene sheet (free PPy particles existed in Fig. 1F) when the amount of pyrrole added exceeded the adsorption capacity of RGO-HP5A. The SEM images of RGO-HP5A-PPy composites shown in Fig. S1 (Supporting information) revealed that free granular PPy was generated outside the graphene sheet when the mass ratio of RGO-HP5A to pyrrole was 1:6. Based on these results, it could be predicted that when the mass ratio of RGO-HP5A and pyrrole added was 1:5, the composite obtained had the highest initial specific capacitance. In addition, the composites could be better infiltrated by aqueous electrolytes when used as electrode materials for supercapacitors, because contact angle tests confirmed the hydrophilicity of these composites (Fig. S2 in Supporting information). The dispersion stability of the composites in water was also investigated (Fig. S3 in Supporting information). Loading PPy onto RGO-HP5A greatly affected the stability of the pillar[5]arene functionalized graphene dispersed in aqueous solution, and the larger the proportion of PPy in the composite, the worse the stability of the aqueous dispersion. Therefore, too much PPy loaded on the graphene would affect the stability of the composites in water systems.

For comparison, the same method was used to synthesize pure PPy, PPy doped with HP5A (HP5A-PPy) and RGO loaded with PPy (RGO-PPy). The morphology of the obtained PPy was granular (Fig. S4 in Supporting information). Compared with HP5A-PPy, the

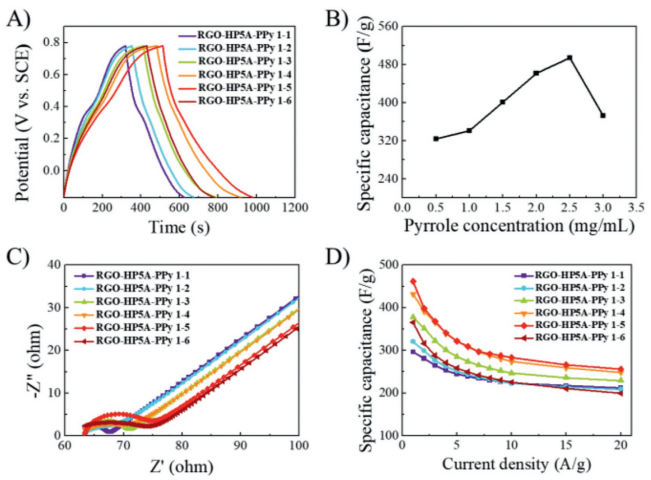

Fig. 2. (A) Charge-discharge curves (1 A/g) of the electrodes modified of RGO-HP5A-PPy 1–1, RGO-HP5A-PPy 1–2, RGO-HP5A-PPy 1–3, RGO-HP5A-PPy 1–4, RGO-HP5A-PPy 1–5 and RGO-HP5A-PPy 1–6. (B) The specific capacitance of the composites obtained by adding different amounts of pyrrole solution. (C) EIS Nyquist plots of RGO-HP5A-PPy modified electrodes. Inset: a modified Randles' equivalent circuit model applied to fit the impedance data. (D) Specific capacitance at various discharge current densities of RGO-HP5A-PPy composites.

Table 1
Physical properties deduced from N_2 adsorption-desorption at 77 K on PPy, RGO-HP5A-PPy 1–4 and RGO-HP5A-PPy 1–5.

Samples	Surface area (m^2/g)	Average pore volume (cm^3/g)	Average pore diameter (nm)
PPy	33.26	0.08	9.67
RGO-HP5A-PPy 1–4	71.04	0.23	12.96
RGO-HP5A-PPy 1–5	52.15	0.17	13.13

size of pure PPy was larger and the agglomeration was more serious. The sheets of RGO-PPy were very thick and the PPy loaded on the RGO was not uniform (Fig. S4C). Part of PPy particles outside the graphene sheet in Fig. S4F revealed that RGO-HP5A had a much better binding ability with PPy than RGO. The prepared materials were also characterized by FT-IR spectra (Fig. S5 in Supporting information), XRD patterns (Fig. S6 in Supporting information), Brunauer-Emmett-Teller (BET) method and the Barrett-Joyner-Halenda (BJH) model (Fig. S7 in Supporting information). PPy had a BET specific surface area of only 33.26 m^2/g, while RGO-HP5A-PPy 1–4 and RGO-HP5A-PPy 1–5 had a larger specific surface area of 71.04 m^2/g and 52.15 m^2/g respectively (Table 1). The small specific surface area of PPy was mainly due to the serious agglomeration of pure PPy. However, PPy was uniformly attached to the graphene surface when it was compounded with RGO-HP5A, causing the agglomeration to be significantly inhibited. As the load of PPy increased, the composite became thicker, resulting in a decrease in the specific surface area. In addition, RGO-HP5A-PPy had a slightly better thermal stability in comparison with pure PPy (Fig. S8 in Supporting information).

The unique structural features resulted in an excellent electrochemical performance of RGO-HP5A-PPy electrodes (Fig. 2 and Fig. S9 in Supporting information). Cyclic voltammetry (CV) curves exhibited that the capacitance of the composites was contributed by electric double layer capacitance and pseudocapacitance [37]. As the added amount of pyrrole increased, it could be observed that the relative intensity of the redox peak attributable to HP5A weakened, while the contribution of the PPy component to the capacitance increased (Fig. S9) Figs. 2A and B clearly revealed that RGO-HP5A-PPy 1–5 had the highest specific capacitance (C_s = 495 F/g) at 1 A/g, followed by RGO-HP5A-PPy 1–4 (C_s = 462 F/g). As the amount of RGO-HP5A was constant, the C_s of the composite was enhanced from 324 F/g to 495 F/g with the increase of pyrrole from 0.5 to 2.5 mg/mL. The improvement in specific capacitance was due to the increase in the loading of PPy, and the inhibition of the aggregation by RGO-HP5A. When the amount of pyrrole continued to increase to 3.0 mg/mL, the C_s decreased to 372 F/g. This was because the amount of pyrrole exceeded the load carrying limit of RGO-HP5A, and the excess pyrrole spontaneously and disorderly agglomerated after polymerization outside of graphene. In general, the C_s of the composites prepared on the basis of RGO-HP5A was significantly higher than that of PPy, HP5A-PPy and RGO-PPy (Fig. S10 in Supporting information).

Then, electrochemical impedance spectroscopy (EIS) was used to characterize the electronic conductivity and ion transport performance of the materials (Fig. 2C and Fig. S11 in Supporting information). The Nyquist plots fitted according to an adjusted Randles' equivalent circuit [38–40] were shown in Fig. 2C. The charge transfer resistance (R_{ct}) of these RGO-HP5A-PPy composites were 5.1, 6.8, 7.1, 8.0, 10.5 and 15.6 Ω, respectively. It could be seen that as the content of PPy in composites increased, the resistance increased, which would influence the rate capability. Compared with PPy (Fig. S12 in Supporting information), the rate capability of RGO-HP5A-PPy composites was observably improved (Fig. 2D and Fig. S13 in Supporting information), which was mainly due to the connection role of HP5A and the support of graphene, improving the conductivity and making the composites more stable during high-current charging and discharging. The C_s retention rates of these RGO-HP5A-PPy composites in 1∼20 A/g were 72%, 65%, 61%, 57%, 55% and 54%, respectively (Fig. 2D). When the loading of PPy increased, the rate capability of the composite decreased, mainly because the increase of organic matter in the composition weakened the conductivity of the material. The amount of pillar[5]arenes on the graphene also affected the performance of the composites (Fig. S14 in Supporting information). Additionally, the RGO-HP5A-PPy composites prevail over many PPy/graphene composites in the literature (Table S2 in Supporting information).

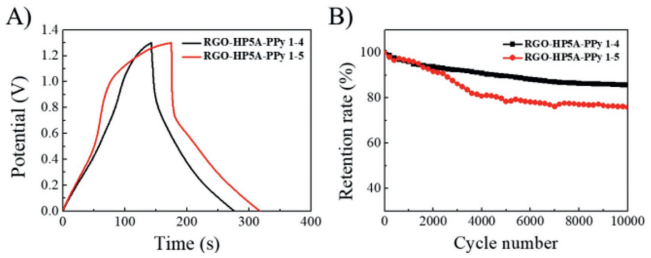

Fig. 3. (A) Galvanostatic charge and discharge curves at 1 A/g, (B) cycling stability over 10,000 cycles at a current density of 5 A/g of the RGO-HP5A-PPy 1–4//RGO-HP5A-PPy 1–4 and RGO-HP5A-PPy 1–5//RGO-HP5A-PPy 1–5 symmetric supercapacitors.

For purpose of evaluating the feasibility of RGO-HP5A-PPy composites in the practical application of supercapacitors, two symmetrical supercapacitors were assembled using RGO-HP5A-PPy 1–4 and RGO-HP5A-PPy 1–5 as active materials. The CV curves of RGO-HP5A-PPy 1–4//RGO-HP5A-PPy 1–4 and RGO-HP5A-PPy 1–5//RGO-HP5A-PPy 1–5 in the potential window of 0∼1.3 V were shown in Fig. S15 (Supporting information). The supercapacitors were subsequently subjected to a galvanostatic charge and discharge test at 1 A/g to evaluate their performance (Fig. 3A). The specific capacitances of the two supercapacitors were calculated to be 103 and 110 F/g, respectively. According to the CV curves of the assembled two supercapacitors at different scan rates (Figs. S16A and C in Supporting information) and the charge-discharge curves at different current densities (Figs. S16B and D in Supporting information), the C_s retention rate of RGO-HP5A-PPy 1–4//RGO-HP5A-PPy 1–4 from 1 A/g to 20 A/g was 71% (Fig. S16E in Supporting information). The C_s retention rate of RGO-HP5A-PPy 1–5//RGO-HP5A-PPy 1–5 from 1 A/g to 20 A/g was 54% (Fig. S16E). According to the obtained Ragone plot [41] shown in Fig. S16F (Supporting information), when the power density was 2340 W/kg, the maximum energy density of the two supercapacitors were 81.7 and 87.0 Wh/kg, respectively; when the power density reached 46,800 W/kg, the energy density remained 58.4 and 47.3 Wh/kg, respectively. Fig. S17 (Supporting information) showed the Nyquist plots of the supercapacitors. It was obvious that the impedance of RGO-HP5A-PPy 1–4//RGO-HP5A-PPy 1–4 was smaller (R_{ct} = 0.4 Ω), which resulted in the better rate capability of RGO-HP5A-PPy 1–4//RGO-HP5A-PPy 1–4. Then, the cyclic stability was investigated at 5 A/g, and the specific capacitance retention rates of the two symmetrical supercapacitors were 86% and 76%, respectively, indicating that the composites had good electrochemical stability (Fig. 3B).

In this paper, hydrophilic RGO-HP5A-PPy composites with thin sheet morphology were obtained by using pillar[5]arene functionalized graphene as substrate and inducing polymerization of pyrrole on graphene surface by the assistance of pillar[5]arenes. Different from the granular morphology of pure PPy, the PPy in the composites covered the graphene surface in the form of a film. RGO-HP5A-PPy 1–5 had the highest specific capacitance (495 F/g at 1 A/g, 55% higher than that of PPy), and its rate capability was much better than that of PPy. The assembled symmetric supercapacitors exhibited a high initial specific capacitance, good rate capability and fine cyclic stability. The research was expected to offer a new model for constructing PPy/graphene hybrid materials and a reference for the development of pillar[*n*]arene functionalized composites in energy storage.

Declaration of competing interest

The authors declare that they have no known competing financial interests or personal relationships that could have appeared to influence the work reported in this paper.

Acknowledgments

This work was supported by the National Natural Science Foundation of China (Nos. 21703200 and 21773203), the Chey Institute for Advanced Studies International Scholar Exchange Fellowship for the academic year of 2021–2022, the Natural Science Foundation of Jiangsu Province of China (No. BK20170485), Postgraduate Research & Practice Innovation Program of Jiangsu Province (Nos. SJCX21_1565 and KYCX21_3204), China Scholarship Council program (No. 201908320084), and the Project Funded by the Priority Academic Program Development of Jiangsu Higher Education Institutions.

Supplementary materials

Supplementary material associated with this article can be found, in the online version, at doi:10.1016/j.cclet.2022.01.088.

References

[1] R.R. Salunkhe, Y.H. Lee, K.H. Chang, Chem. Eur. J. 20 (2014) 13838–13852.
[2] J.R. Miller, P. Simon, Science 321 (2008) 651–652.
[3] L. Lyu, K. Seong, D. Ko, et al., Mater. Chem. Front. 3 (2019) 2543–2570.
[4] M.L. Wang, T.Y. Zhang, M.Z. Cui, et al., Chin. Chem. Lett. 32 (2021) 1111–1116.
[5] Q.F. Meng, K.F. Cai, Y.X. Chen, et al., Nano Energy 36 (2017) 268–285.
[6] Y.Q. Wang, Y. Ding, X.L. Guo, et al., Nano Res. 12 (2019) 1978–1987.
[7] M.L. Wang, Y.F. Yu, M.Z. Cui, et al., Electrochim. Acta 329 (2020) 135181.
[8] P. Naskar, A. Maiti, P. Chakraborty, et al., J. Mater. Chem. A 9 (2021) 1970–2017.
[9] Y.Z. Zhao, Y.M. Cai, Y. Wang, et al., Sep. Purif. Technol. 259 (2021) 118175.
[10] H. Zhuo, Y.J. Hu, Z.H. Chen, et al., Carbohyd. Polym. 215 (2019) 322–329.
[11] A. Ehsani, A.A. Heidari, H.M. Shiri, Chem. Rec. 19 (2019) 908–926.
[12] I.J. Gómez, M.V. Sulleiro, D. Mantione, et al., Polymers (Basel) 13 (2021) 745.
[13] R.B. Choudhary, S. Ansari, B. Purty, J. Energy Storage 29 (2020) 101302.
[14] R. Zhang, H. Pang, J. Energy Storage 33 (2021) 102037.
[15] J.H. Zhao, J.P. Wu, B. Li, et al., Prog. Nat. Sci. 26 (2016) 237–242.
[16] T.F. Yi, L.Y. Qiu, J. Mei, et al., Sci. Bull. 65 (2020) 546–556.
[17] B.C. Kim, J.Y. Hong, G.G. Wallace, et al., Adv. Energy Mat. 5 (2015) 1500959.
[18] L.B. Ni, W. Zhang, Z. Wu, et al., Appl. Surf. Sci. 396 (2017) 412–420.
[19] B. Wang, T.T. Ruan, Y. Chen, et al., Energy Storage Mater 24 (2020) 22–51.
[20] D. Nandi, V.B. Mohan, A.K. Bhowmick, et al., J. Mater. Sci. 55 (2020) 6375–6400.
[21] Ni L.B, G. Yang, C.Y. Sun, et al., Mater. Today Energy 6 (2017) 53–64.
[22] A.G. Olabi, M.A. Abdelkareem, T. Wilberforce, et al., Renew. Sust. Energ. Rev. 135 (2021) 110026.
[23] M.L. He, L.J. Chen, B. Jiang, et al., Chin. Chem. Lett. 30 (2019) 131–134.
[24] Y. Han, C.Y. Nie, S. Jiang, et al., Chin. Chem. Lett. 31 (2020) 725–728.
[25] Y. Cai, Z.C. Zhang, Y. Ding, et al., Chin. Chem. Lett. 32 (2021) 1267–1279.
[26] C. Peng, W.T. Liang, J.C. Ji, et al., Chin. Chem. Lett. 32 (2021) 345–348.
[27] J. Zhou, M. Chen, J. Xie, et al., ACS Appl. Mater. Interfaces 5 (2013) 11218–11224.
[28] F. Guo, P. Xiao, B.Y. Yan, et al., Chem. Eng. J. 391 (2020) 123511.
[29] Y. Gao, Nanoscale Res. Lett. 12 (2017) 387.
[30] J.P. Wang, X. Li, X.F. Du, et al., Chem. Pap. 71 (2017) 293–316.
[31] W.L. Wu, L.Q. Yang, S.L. Chen, et al., RSC Adv. 5 (2015) 91645–91653.
[32] S.Z. Xu, H.L. Hao, Y.N. Chen, et al., Nanotechnology 32 (2021) 305401.
[33] S. Kulandaivalu, N. Suhaimi, Y. Sulaiman, Sci. Rep. 9 (2019) 4884.
[34] Y.K. Kim, K.Y. Shin, Appl. Surf. Sci. 547 (2021) 149141.
[35] R. Montecinos, F. Diaz-Wilson, A. Bravo-Sepulveda, et al., J. Phys. Org. Chem. 32 (2019) e3889.
[36] W. Zhang, Y.Y. Kong, X.Z. Jin, et al., Electrochim. Acta 331 (2020) 135345.
[37] Y.Z. Fang, B.W. Yang, D.T. He, et al., Chin. Chem. Lett. 31 (2020) 1004–1008.
[38] J.J. Jiang, X.Y. Lin, G.W. Diao, ACS Appl. Mater. Interfaces 3 (2017) 36688–36694.
[39] F.B. Ajdari, E. Kowsari, A. Ehsani, J. Solid State Chem. 265 (2018) 155–166.
[40] F.B. Ajdari, E. Kowsari, A. Ehsani, et al., Electrochim. Acta 292 (2018) 789–804.
[41] W. Zhang, X.Z. Jin, H. Chai, et al., Adv. Mater. Interfaces 5 (2018) 1800106.